ORIGINAL ARTICLE

Establishment of a Treatment Method for Peri-Implantitis Using Bio-Apatite Peening

Hideaki SATO[1], Chihiro MOCHIZUKI[2], Sora OHBA[1], Yutaka KAMEYAMA[1], Shuhei KODAMA[1], Yishen XIE[3], Akane OMORI[4], and Satoshi KOMASA[4]

[1]Department of Mechanical Engineering, Faculty of Science and Engineering, Tokyo City University, Tokyo, Japan
[2] BIOAPATITE, INC. Shiga, Japan
[3]Department of Oral Health Engineering, [4]Department of Oral Health Sciences, Faculty of Health Sciences, Osaka Dental University, Osaka, Japan

Synopsis
Peri-implantitis is characterized by inflammation and progressive bone loss around dental implants. Because bacterial contamination of complex implant surfaces makes re-osseointegration difficult after conventional debridement, surface treatment methods that achieve both decontamination and biofunctionalization are required. This study aimed to investigate a novel approach using bio-apatite particle peening to simultaneously clean and transfer bio-apatite onto pure titanium surfaces. Bio-apatite particles derived from eggshells were peened onto commercially pure titanium under controlled conditions (pressure: 0.6 MPa, particle mass flow rate: 1 g/s, nozzle distance: 20 mm). The transfer behavior, cleaning efficiency, and biological responses were evaluated using mass measurements, EDS analysis, optical microscopy, and cell culture experiments. The results showed that bio-apatite was successfully peened onto titanium surfaces, and the transfer amount increased with increasing particle peening quantity. Artificial plaque was effectively removed, while bio-apatite transfer occurred simultaneously. EDS analysis confirmed increased Mg content, indicating successful transfer of bio-apatite. Cell experiments revealed enhanced osteoblast adhesion, ALP activity, DNA content, and calcium deposition on bio-apatite-transferred surfaces, especially with higher peening amounts. These findings suggest that bio-apatite particle peening is a promising technique for implant surface modification, enabling simultaneous cleaning and biofunctionalization to enhance osteogenic potential.

Key words*: bio-apatite, peri-implantitis, peening, cleaning, transfer*

Introduction

Implant therapy has established itself as an effective treatment for restoring function lost due to missing teeth. However, despite advances in implant therapy, peri-implantitis remains a growing concern in dental practice [1-5]. Peri-implant diseases include peri-implantitis and peri-implant mucositis. Peri-implantitis is an inflammatory disease accompanied by bone destruction, whereas peri-implant mucositis is a reversible inflammation limited to the surrounding mucosal tissue and does not involve bone resorption [6-8]. Even implants that have been properly diagnosed, placed, and achieved osseointegration to allow for functional occlusion can develop peri-implant diseases if maintenance is inadequate.

Peri-implant diseases are a collective term for conditions in which bacterial infection around the implant induces inflammation of the surrounding soft tissue, leading to bone destruction [9-11]. The primary goal in treating peri-implantitis is to reduce inflammation at the affected site, as the disease is caused by bacterial

infection [2, 5, 9, 12]. Anti-inflammatory treatments are based on fundamental periodontal therapy and may include plaque control, debridement, sterilization, antimicrobial therapy, and occlusal adjustment, with intervention tailored to the symptoms.

After anti-inflammatory treatment, re-evaluation is performed to determine, depending on the symptoms, the suitability of surgical or non-surgical procedures. Previous reviews and clinical studies have indicated that non-surgical procedures alone generally show limited effectiveness for peri-implantitis, particularly in cases with advanced bone loss, and that re-osseointegration around contaminated implant surfaces remains difficult to achieve [13-15]. This is mainly because debridement of the contaminated implant surface is extremely challenging, given its texture and threads. Therefore, a variety of current treatments for peri-implantitis are commonly used, including Er:YAG lasers, air-powder abrasion with various powders, mechanical cleaning with hand or ultrasonic scalers, chemical cleaning with agents such as phosphoric acid or chlorhexidine, or combinations of these methods [16-21]. In our previous report, we focused on verifying air-powder abrasion using various particles. We clarified that agar particles are useful for cleaning contaminated implant surfaces without damaging the implant material surface [22]. However, cleaning with agar particles after peri-implantitis treatment is insufficient to achieve re-osseointegration, and it is essential to develop methods that enable cleaning of the contaminated implant surface and the early re-acquisition of osseointegration.

We have focused on hydroxyapatite derived from eggshells, which was developed by bio-apatite (hereafter referred to as bio-apatite) [23]. Bio-apatite is hydroxyapatite created by recovering calcium from discarded eggshells, which are considered food waste [23]. Bio-apatite can be prepared without the use of buffering agents, solvents, or catalysts using a unique method and apparatus to separate eggshells from their membranes and pulverize the shells into microcrystals. Bio-apatite is non-toxic to the human body and, owing to its protein-adsorbing ability, has already been commercialized as a plaque-removing component in toothpaste. Moreover, measurements of calcification degree suggest that it also has the potential to promote remineralization [24, 25]. Furthermore, because bio-apatite contains Mg ions, which are essential inorganic ions involved in enzymatic reactions and bone metabolism and are known to show low toxicity as inorganic elements, high biocompatibility is expected; previous reports also suggest that Mg-containing biomaterials can enhance hard-tissue differentiation [24, 25, 38, 39]. The bio-apatite particles used in this study were small, with a mean circle-equivalent diameter of 2.32 μm. Therefore, similar to agar particles, it is surmised that, when peened onto a material surface, they may clean contaminated implant surfaces without damaging the material.

We considered whether peening bio-apatite particles onto contaminated implant surfaces could clean the surface and whether the transferred bio-apatite could promote re-osseointegration. Therefore, in this study, we examined the cleaning efficacy on material surfaces and the impact on biocompatibility after cleaning by peening bio-apatite particles onto pure titanium plates with artificial plaque, a commonly used mock contaminant.

Materials and Methods

Peening Apparatus

Figure 1 shows a schematic of the peening apparatus. Figure 2 shows the airflow in the experimental apparatus. Using a compressor, air is compressed and stored in a tank. A pressure-reducing valve is connected to the tank to maintain a constant air pressure. The pressure-regulated air is fed through a nozzle to perform peening. A shot-peening nozzle (Fuji Manufacturing Co., Ltd., Tokyo, Japan) was used in this study.

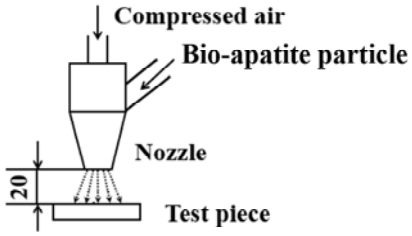

Figure 1 Peening apparatus

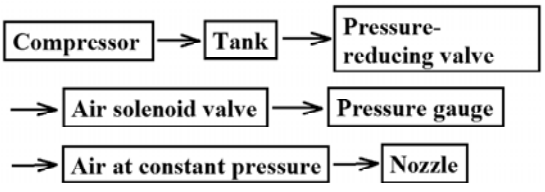

Figure 2 Airflow

Particles and Test Specimens

Bio-apatite was prepared from discarded eggshells by separating the shell membrane, washing and drying the shells, pulverizing them into microcrystals, and converting the calcium source into sulfate-free apatite without using buffering agents, solvents, or catalysts, according to the manufacturer's process and a previously described method [23]. The particles were supplied as sulfate-free apatite derived from eggshells (Bio-apatite ($Ca_{9.3}Mg_{0.7}(PO_4)_6(OH)_2$); Bio-apatite- Medical, BIOAPATITE Inc., Hikone, Shiga, Japan). Figure 3 shows the morphology of the bio-apatite particles, measured using a Morphologi 4 (Malvern Panalytical, Tokyo, Japan). The mean circle-equivalent diameter of the bio-apatite particles was 2.32 μm. The test specimen was a titanium disk. Titanium disks (diameter: 15 mm; thickness: 1 mm) of JIS grade 2 pure titanium (Kobe Steel, Ltd., Kobe, Japan) were fabricated by cutting and polishing. The disks were polished with waterproof silicon carbide (SiC) abrasive paper (grain sizes No. #400, #600, #800, #1,000, and #1,200; SANKYO RIKAGAKU CO., LTD., Okegawa, Saitama, Japan), ultrasonically rinsed in acetone, ethanol, and distilled water for 10 min each, and air-dried. The arithmetic mean surface roughness (Ra) of the test specimen surface was adjusted to a range of 0.10 μm to 0.17 μm. Disk-shaped test specimens were used for surface observation and bioactivity evaluation.

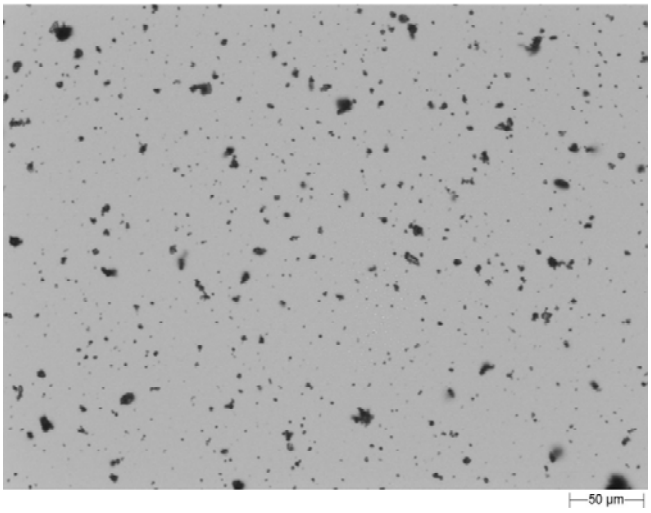

Figure 3 Bio-apatite particles measured by Morphologi 4. The mean circle-equivalent diameter was 2.32 μm.

Experimental Conditions and Evaluation Methods

Bio-apatite was peened onto the pure titanium test specimens at a perpendicular projection angle using the aforementioned peening apparatus under the peening conditions listed in Table 1. The peening pressure, particle mass flow rate, nozzle distance, and total particle mass were controlled as experimental conditions. The surface morphologies and elemental distributions of the specimens were observed using scanning electron microscopy (SEM; Miniscope TM3000; Hitachi High-Tech Corporation, Tokyo, Japan) and energy-dispersive X-ray spectroscopy (EDS). The mass of each titanium disk was measured before and after bio-apatite peening using an electronic balance (GX-324A; A&D Company, Limited, Tokyo, Japan), and the transfer mass was calculated by subtracting the pre-peening mass from the post-peening mass. Each condition was measured in triplicate.

Table 1 Peening conditions

Test piece	Pure titanium
Particle	Bio-apatite
Pressure *P*	0.6MPa
Nozzle distance *L*	20mm
Number of peening	1 times
Particle mass flow rate	1g/s
Total particle mass	10g, 20g, 30g

Adhesion Assessment Following Artificial Plaque Removal

Artificial plaque (NISSIN Dental Products Inc., Kyoto, Japan) was used as a simulated stain. The main component of the artificial plaque is silicon dioxide. Bio-apatite was peened onto the titanium test specimens after coating artificial plaque at a perpendicular peening angle using the aforementioned peening apparatus under the peening conditions listed in Table 1. The detailed peening conditions, including peening pressure, particle mass flow rate, nozzle distance, and total particle mass, were the same as those described above. The effects of bio-apatite peening on the surface of a pure titanium plate coated with artificial plaque were observed using an optical microscope and SEM/EDS. Subsequently, the material was evaluated in vitro using rat bone marrow cells.

Cell culture

Rat bone marrow (RBM) cells were isolated from the femurs and tibiae of three eight-week-old Sprague–Dawley rat. This study was approved by the Guidelines for Animal Experimentation of Osaka Dental University (approval no. 23–11001). The rat was euthanized by 4% isoflurane inhalation, and the bones were aseptically excised from the hind limbs. The proximal ends of the femurs and the distal ends of the tibiae were clipped and flushed with Eagle's minimal essential medium (MEM; Wako Pure Chemical Industries Ltd., Osaka, Japan). A 21-gauge needle (Terumo Corp., Tokyo, Japan) was used to aspirate the bone marrow. The marrow pellets were dispersed by trituration. Cell suspensions from all bones were combined in one centrifuge tube. The RBM cells were cultured in 75-cm^2 Falcon culture flasks (BD Biosciences, Franklin Lakes, NJ, USA) at 37 °C under a 5% CO_2 atmosphere in a growth medium containing MEM supplemented with 10% fetal bovine serum (FBS; Invitrogen/Life Technologies, Carlsbad, CA, USA), penicillin (500 U mL^{-1}; Cambrex Bio Science, Walkersville, MD, USA), and Fungizone (1.25 μg mL^{-1}; Cambrex Bio Science, Walkersville, MD, USA). The cells reached confluence after approximately 7 d of culture. The cells reached confluence after approximately 10 days of culture. When the cells reached confluence, they were removed from the flask by trypsinization, washed twice with phosphate-buffered saline (PBS), resuspended in culture medium, and seeded at a density of 4×10^4 cm^{-2} in 24-well Falcon tissue culture plates (BD Biosciences, Franklin Lakes, NJ, USA) containing either a test or a control titanium disk. For ALP activity and mineralization assays, osteogenic differentiation was induced using MEM supplemented with 10% FBS, antibiotics, 50 μg/mL ascorbic acid, 10 mM β-glycerophosphate, and 10 nM dexamethasone.

Cell Adhesion

Cell adhesion was measured using a Cell Titer-Blue Cell Viability Assay Kit (Promega, Madison, WI, USA) according to the manufacturer's protocol. RBM cells were seeded onto the samples at a density of 4×10^4 cells/cm^2 and allowed to attach for 3 and 24 h. At each time point, the non-adherent cells were removed by rinsing with PBS. CellTiter-Blue Reagent (50 μL) and PBS (250 μL) were then added to each well. After incubation at 37 °C for 1 h, the solution was removed, and 3 × 100 μL (triplicate) of it was transferred to a new Falcon 96-well tissue culture plate (BD Biosciences, Franklin Lakes, NJ, USA). The absorbance of the remaining solution was measured at OD560/590.

ALP activity

RBM cells at 7 and 14 d culture were washed with PBS and lysed with 200 μL of 0.2% Triton X-100 (Sigma-Aldrich, St. Louis, MO, USA). The lysate was transferred to a microcentrifuge tube containing a hardened 5-mm steel ball. The tube was agitated on a shaker (Mixer Mill Type MM 301; Retsch GmbH, Haan, Germany) at 29 Hz for 20 s to homogenize the contents. ALP activity was measured with an alkaline phosphatase luminometric enzyme-linked immunosorbent assay (ELISA) kit (Sigma-Aldrich, St. Louis, MO, USA) according to the manufacturer's protocol. The reaction was terminated by adding 3 N NaOH until a final concentration of 0.5 N NaOH was achieved. Then, *p*-nitrophenol production was determined on a microplate reader (Molecular Devices, Sunnyvale, CA, USA). DNA content was measured with a PicoGreen dsDNA assay kit (Invitrogen/Life Technologies, Carlsbad, CA, USA) according to the manufacturer's protocol. The amount of ALP was normalized to the amount of DNA in the cell lysate.

Mineralization

Mineralization was assessed using a calcium E-test kit (Wako Pure Chemical Industries Ltd., Osaka, Japan). RBM cells were cultured in osteogenic differentiation medium as described above. At each time point (21 or 28 d), 1 mL of calcium E-test reagent and 2 mL of buffer were added to 50 μL of medium. The absorbance of the reaction products was measured at 610 nm in a 96-well microplate reader (SpectraMax M5; Molecular Devices, Sunnyvale, CA, USA). The calcium ion concentration was calculated from the absorbance value relative to a standard curve.

Statistical Analysis

Characterization analyses and in vitro experiments were performed in triplicate. Statistical analyses were conducted using GraphPad Prism 9.0 software, and the degree of statistical significance was assessed via one-way analysis of variance, followed by Bonferroni's post hoc test. All quantitative results are presented as the mean ± standard deviation, and $p < 0.05$ was considered statistically significant, whereas $p < 0.01$ was considered highly statistically significant.

Results

Adhesion Results with Bioapatite

Figure 4 shows the EDS elemental mapping results obtained after bio-apatite peening at a total particle mass of 10 g. The color maps indicate the distribution of each detected element, and O-KA, Mg-K, P-KA, Ca-KA, and Ti-K represent the characteristic Kα X-ray signals for oxygen, magnesium, phosphorus, calcium, and titanium, respectively. These observations revealed the presence of Mg, Ca, and P, which are components of bio-apatite, on the surface of the pure titanium plate, confirming that bio-apatite had been transferred to the surface. Figure 5 shows optical microscope images taken at 200× magnification after bio-apatite peening with total particle masses of 10 g and 20 g. Representative images from triplicate specimens are shown for

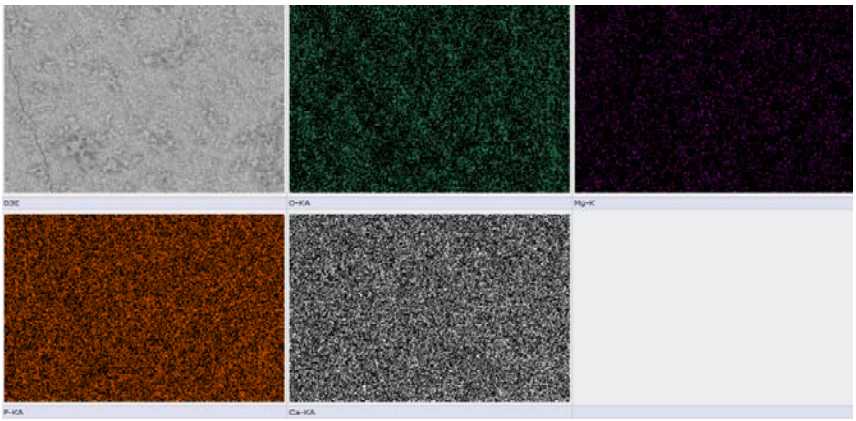

Figure 4 EDS elemental mapping following bio-apatite peening (total particle mass: 10 g). O-KA, Mg-K, P-KA, Ca-KA, and Ti-K indicate the characteristic Kα X-ray signals for oxygen, magnesium, phosphorus, calcium, and titanium, respectively.

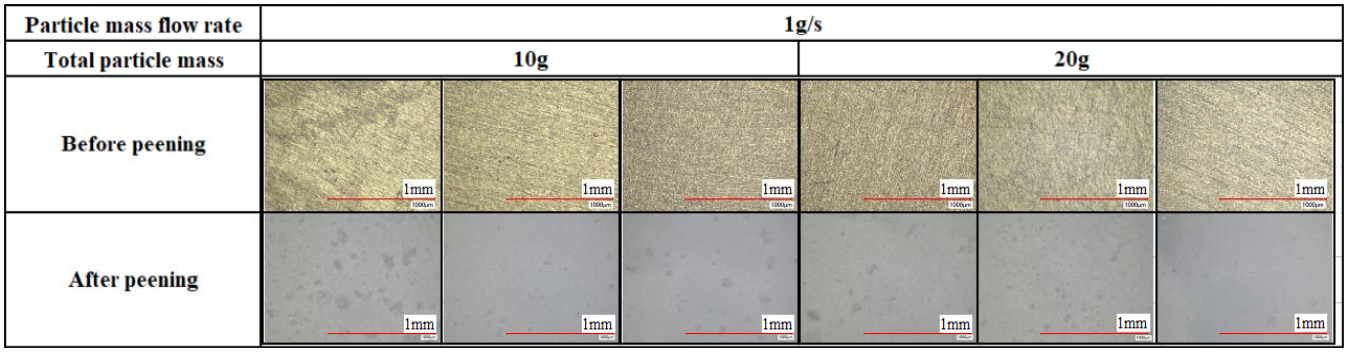

Figure 5 Bio-apatite peening results at total particle masses of 10 g and 20 g. Representative optical microscope images from triplicate specimens are shown for each condition.

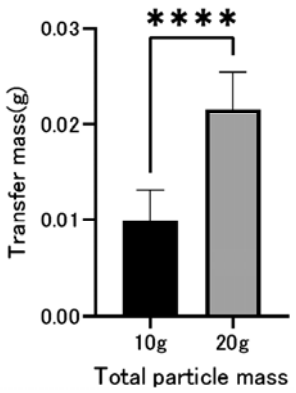

Figure 6 Transfer mass of bio-apatite peening. The mass of each titanium disk was measured before and after peening, and the transfer mass was calculated as the post-peening mass minus the pre-peening mass (n = 3).

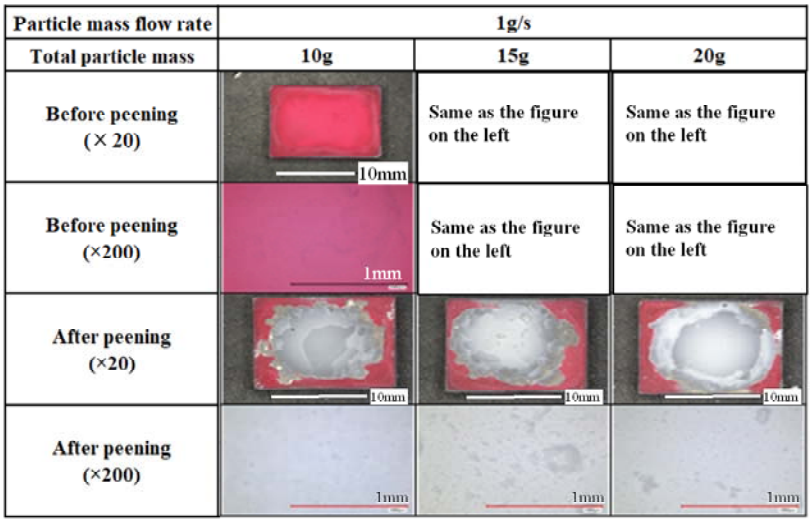

Figure 7 Bio-apatite peening results with artificial plaque. Images before peening show titanium surfaces coated with artificial plaque, and images after peening show plaque removal and bio-apatite transfer under each peening condition.

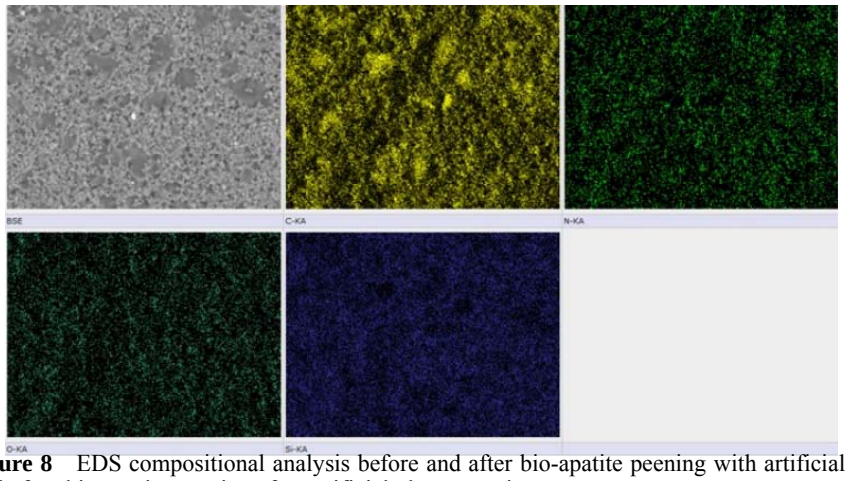

Figure 8 EDS compositional analysis before and after bio-apatite peening with artificial plaque: (a) before bio-apatite peening after artificial plaque coating

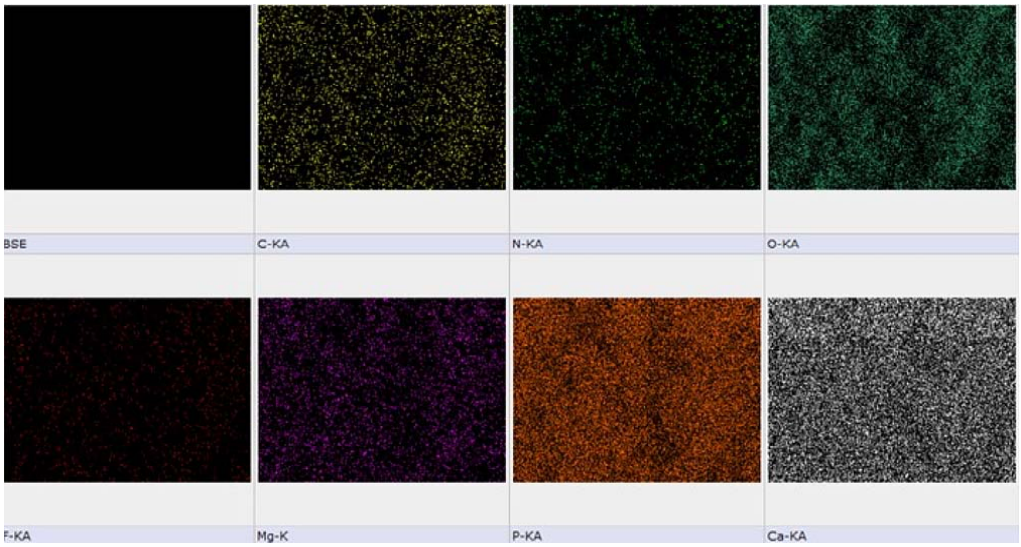

(b) after bio-apatite peening at total particle mass 10 g

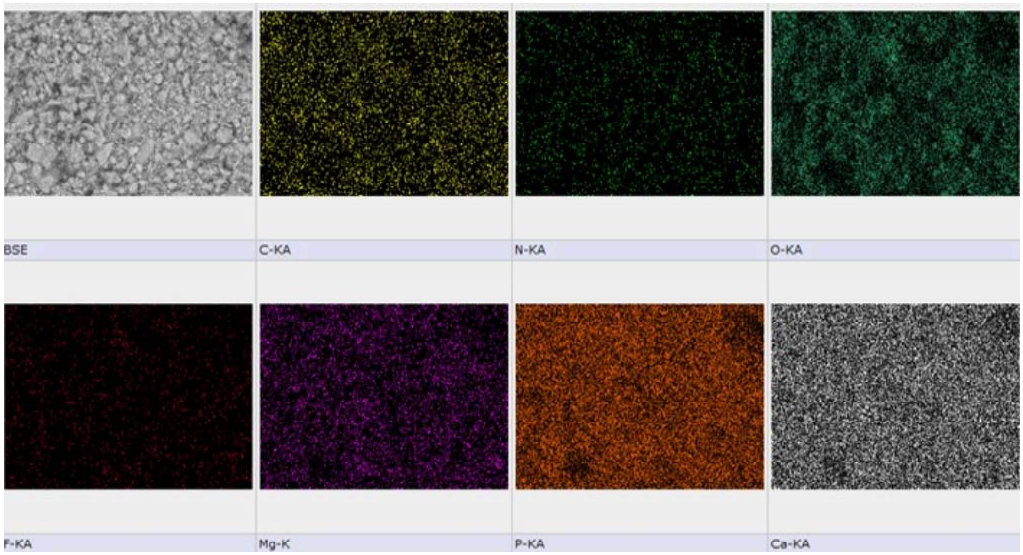

(c) after bio-apatite peening at total particle mass 20 g

each condition. At both 10 g and 20 g total particle mass, white transferred areas were observed on the titanium surface, and the transferred area was more extensive under the 20 g condition. Figure 6 shows the results of the transfer mass measurements obtained from mass analysis. An average deposition of 0.009964 g was observed at a total particle mass of 10 g, and 0.021573 g at 20 g, clearly indicating that the transfer mass was higher at 20 g.

Transfer and Cleaning Using Bio-apatite Peening

Figure 7 shows optical microscope images at 20× and 200× magnification before and after bio-apatite peening. The images before peening show titanium surfaces coated with artificial plaque, and the images after peening show the treated areas under each total particle mass condition. Bio-apatite peening removed the artificial plaque. Furthermore, bio-apatite was transferred to the surface of the pure titanium plate. It is also evident that increasing the total particle mass resulted in a larger cleaned area. Figure 8(a), (b), and (c) shows the EDS compositional analysis before bio-apatite peening after artificial plaque coating, after bio-apatite peening at a total particle mass of 10 g, and after bio-apatite peening at a total particle mass of 20 g, respectively. The EDS analysis results indicate that the Si content derived from the artificial plaque decreased after peening, whereas the Mg, Ca, and P contents derived from bio-apatite increased. This suggests that bio-apatite peening cleaned the artificial plaque while bio-apatite was transferred to the surface. Furthermore, Mg concentration increased with total particle mass.

In vitro analysis

RBM cell adhesion to the sample disks was evaluated after 3 and 24 h of incubation. Figure 9 shows the results of the cell adhesion assay. In the bio-apatite peened group, significantly higher cell adhesion counts were observed at all measurement time points compared to the untreated group. Furthermore, the highest cell adhesion count was observed in the 20 g peened total particle mass group. Figure 10 shows the results of the ALP activity. In the bio-apatite peened group, ALP activity was significantly higher at all measurement time points compared to the untreated group. Furthermore, the highest ALP activity was observed in the 20 g peened total particle mass group. Figure 11 shows the results of the Calcium (Ca) deposition analysis. In the bio-apatite peened group, significantly higher Ca deposition was observed at all measurement time points compared to the untreated group. Furthermore, the highest Ca deposition was observed in the 20 g peened total particle mass group.

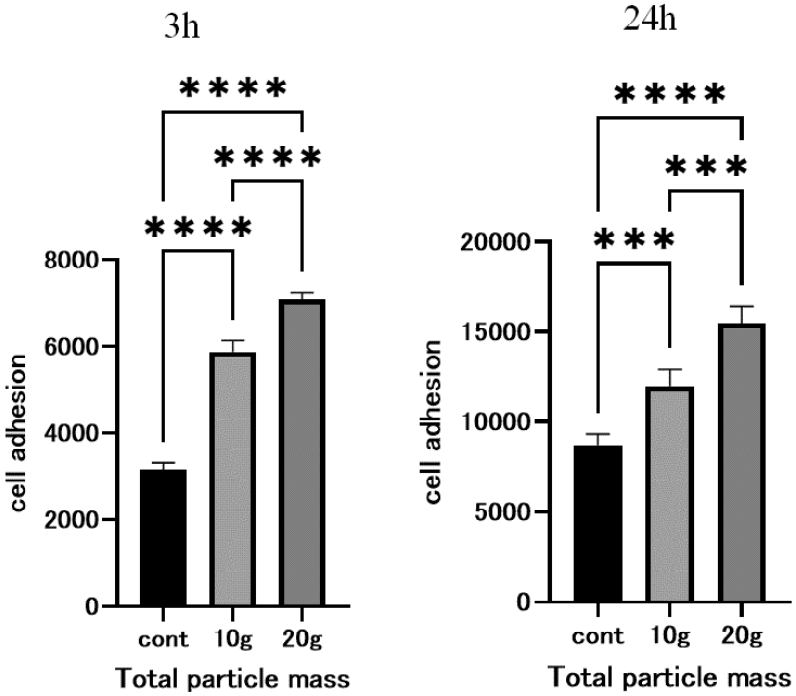

Figure 9 Cell adhesion of RBM cells on titanium disks after 3 and 24 h of culture.

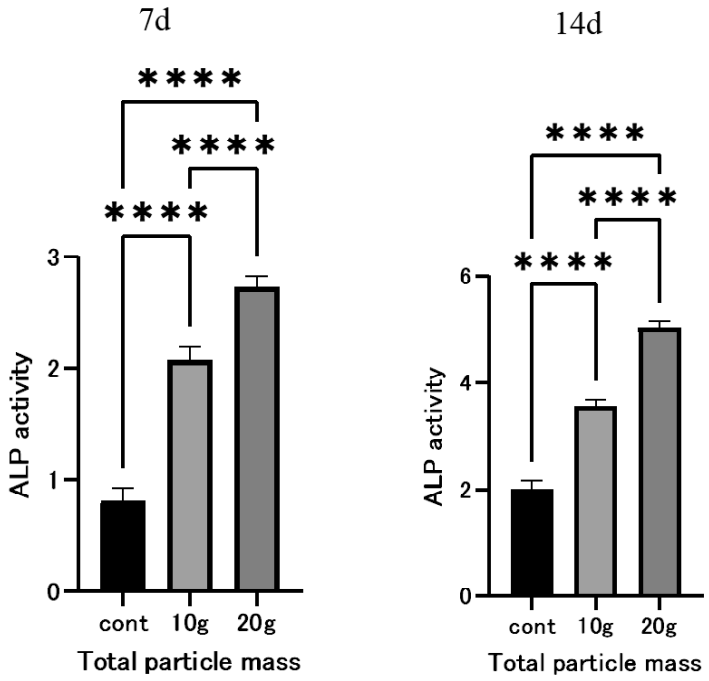

Figure 10 ALP activity of RBM cells on titanium disks after 7 and 14 d of culture.

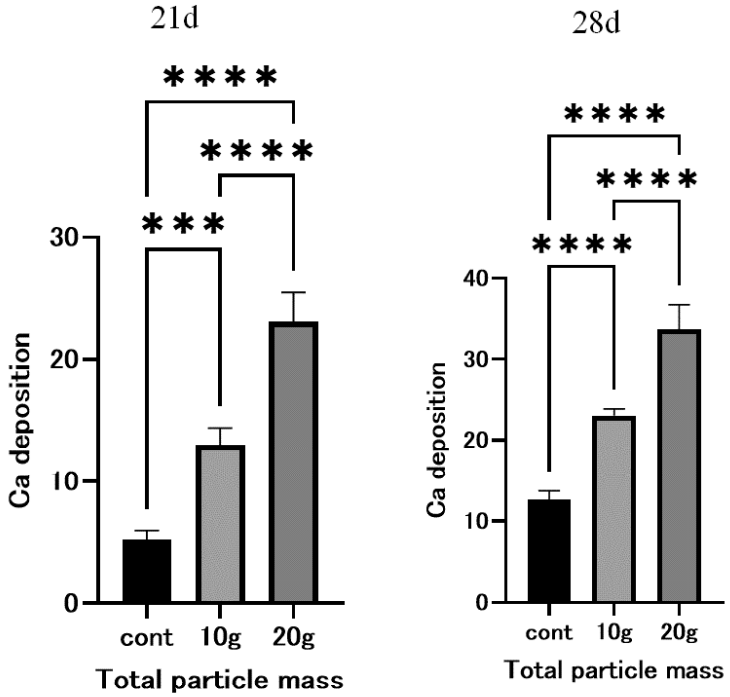

Figure 11 Calcium deposition of RBM cells on titanium disks after 21 and 28 d of culture.

Discussion

The present study demonstrated that bio-apatite particle peening can simultaneously remove artificial plaque and transfer bio-apatite onto titanium surfaces. This dual function is clinically relevant because peri-implantitis treatment requires not only decontamination of the implant surface but also the re-establishment of a biologically favorable interface for re-osseointegration. A central finding of this study is the simultaneous occurrence of effective surface cleaning and bio-apatite transfer on titanium surfaces. Elemental analysis demonstrated a clear increase in the Mg content following

treatment, confirming the successful transfer and retention of bio-apatite particles on the surface. Importantly, the transfer amount increased with increasing total particle mass, suggesting that this technique offers a controllable and scalable means of tailoring surface properties.

This controllability represents a significant advantage over conventional methods, which typically require multiple sequential procedures to achieve decontamination and surface modification independently. The ability to achieve concurrent decontamination and functionalization distinguishes this method from existing peri-implantitis treatments. [28-30]. Conventional approaches, including mechanical debridement, air-powder abrasion, laser irradiation, and chemical disinfection, primarily aim to remove contaminants but do not confer bioactivity to the treated surface.[26-28, 31-33]. Consequently, even after successful decontamination, the re-establishment of a biologically favorable interface remains unpredictable. In contrast, the present findings demonstrate that bio-apatite particle peening not only effectively removes artificial plaque, as evidenced by reduced Si content, but also deposits a bioactive layer that enhances cellular responses. This dual functionality may represent a paradigm shift in the management of peri-implant diseases. The cleaning efficiency observed in this study can be attributed to the physicochemical properties of the bio-apatite particles, particularly their small size (2.32μm) and low abrasiveness [34, 35].

These properties enable efficient removal of contaminants while minimizing damage to the titanium surface. Since significant changes in the surface integrity of implants can adversely affect osseointegration, maintaining surface integrity is of the utmost importance.

Previous studies using larger or more abrasive grains have reported surface damage as a potential drawback of air-abrasion techniques [36]. In this context, bio-apatite particles appear to provide an optimal balance between cleaning efficacy and surface preservation, thereby enhancing their clinical applicability. In addition to surface cleaning, the biological advantages of bio-apatite peening were demonstrated through *in vitro* analyses. The significant enhancement of cell adhesion observed at all time points indicates that the modified surface provides a more favorable microenvironment for initial cell attachment [37]. Because early cell adhesion is a prerequisite for subsequent proliferation and differentiation, this finding suggests that bio-apatite-peened surfaces may facilitate the early stages of osseointegration. The improved cellular response may be attributed to several factors, including increased surface hydrophilicity, enhanced protein adsorption, and the presence of biologically active ions. In particular, the role of Mg ions warrants attention. Magnesium plays a critical role in bone metabolism and influences cellular activities, such as adhesion, proliferation, and differentiation [38, 39]. The incorporation of Mg into the bio-apatite structure may contribute to the observed enhancement in osteoblastic activity. Indeed, the significant increase in ALP activity observed in this study supports the notion that bio-apatite promotes early osteogenic differentiation. The dose-dependent increase in ALP activity further underscores the importance of the transfer quantity as a key parameter in optimizing biological outcomes.

Furthermore, the increased calcium deposition observed at later time points provides strong evidence of enhanced mineralization on bio-apatite-peened surfaces. Mineralization is a hallmark of mature osteoblast function and a critical step in bone formation [40, 41]. The ability of bio-apatite-peened surfaces to promote this process suggests that the treatment accelerates not only early cellular events but also supports the progression toward functional bone tissue formation. This is particularly relevant in the context of peri-implantitis, where bone regeneration is essential to restore implant stability. An additional strength of this study is the use of eggshell-derived bio-apatite as a functional material. From both environmental and economic perspectives, this approach is highly advantageous.

Eggshells, typically considered waste, are a sustainable and abundant source of calcium. The ability to produce bio-apatite without hazardous chemicals further enhances its appeal as a biocompatible, eco-friendly biomaterial. Moreover, the inherent composition of bio-apatite, including trace elements such as Mg, may confer superior biological performance compared to conventional synthetic hydroxyapatite.

While these results are useful, several issues prevent their clinical application. Firstly, the experimental model uses a flat titanium disc, which does not fully reproduce the complex shapes and surface characteristics of clinical implant instruments. The threads and fine surface roughness of the implants can affect both particle transfer and cleaning efficiency. Therefore,

future studies should investigate the applicability of this technique to clinically relevant implant designs. Second, the use of artificial plaque as a model contaminant does not fully capture the structural and biological complexity of mature biofilms associated with peri-implantitis. Real biofilms consist of multispecies microbial communities embedded in extracellular polymeric substances, which can confer resistance to mechanical and chemical removal. Consequently, further studies using established biofilm models are necessary to validate the clinical efficacy of this approach. Third, although the in vitro results provide compelling evidence of enhanced osteogenic potential, *in vivo* validation is essential. The biological environment *in vivo* is considerably more complex, involving immune responses, vascularization, and mechanical loading. These factors may influence both the stability of the bio-apatite-peened surface and its biological performance. Animal studies and clinical trials will be critical to confirm the translational potential of this technique.

In summary, this study presents a novel and clinically relevant approach to implant surface treatment by combining effective decontamination with simultaneous biofunctionalization. By enhancing the physicochemical and biological properties of the implant surface, bio-apatite particle peening offers a promising strategy to overcome the limitations of current peri-implantitis therapies. This integrated approach has the potential to redefine treatment paradigms and improve long-term clinical outcomes in implant dentistry.

Conclusion

Within the scope of this study, we conclude that bio-apatite particle peening enabled simultaneous decontamination and biofunctionalization of titanium surfaces. The method effectively removed artificial plaque and transferred bio-apatite in a controllable manner. Bio-apatite-peened surfaces significantly enhanced cell adhesion, osteogenic differentiation, and mineralization, indicating strong potential to promote early osseointegration. This dual-function approach overcomes the limitations of conventional peri-implantitis treatments that focus solely on decontamination. Therefore, bio-apatite particle peening is a promising strategy for improving the implant surface bioactivity and clinical outcomes. Further in vivo validation is required to confirm its long-term efficacy.

Acknowledgments

We are grateful to the members of Tokyo City University and the Department of Oral Health Engineering at Osaka Dental University for their constructive advice and assistance.

Conflicts of interest

The authors declare that they have no conflicts of interest in this study.

References

1) Heitz-Mayfield LJA. Peri-implant mucositis and peri-implantitis: key features and differences. Br Dent J 2024; 236: 791-794.
2) Schminke B, Vom Orde F, Gruber R, Schliephake H, Bürgers R, Miosge N. The pathology of bone tissue during peri-implantitis. J Dent Res 2014; 94: 354–361.
3) Mordini L, Sun N, Chang N, De Guzman J-P, Generali L, Consolo U. Peri-implantitis regenerative therapy: a review. Biology. 2021; 10: 773. DOI:10.3390/biology10080773
4) Yu Y-M, Lu Y-P, Zhang T, Zheng Y-F, Liu Y-S, Xia D-D. Biomaterials science and surface engineering strategies for dental peri-implantitis management. Mil Med Res 2024; 11(1): 29. doi: 10.1186/s40779-024-00532-9.
5) Poli PP, Cicciu M, Beretta M, Maiorana C. Peri-implant Mucositis and peri-implantitis: a current understanding of their diagnosis, clinical implications, and a report of treatment using a combined therapy approach. J Oral Implantol 2016; 43: 45-50.
6) Nguyen‐Hieu T, Borghetti A, Aboudharam G. Peri‐implantitis: from diagnosis to therapeutics. J Investig Clin Dent 2012; 3: 79-94.
7) Ahn D-H, Kim H-J, Joo J-Y, Lee J-Y. Prevalence and risk factors of peri-implant mucositis and peri-implantitis after at least 7 years of loading. J Periodontal Implant Sci 2019; 49: 397-405. doi: 10.5051/jpis. 2019. 49.6.397.
8) Ogata Y, Nakayama Y, Tatsumi J, Kubota T, Sato S, Nishida T, Takeuchi Y, Onitsuka T, Sakagami R, Nozaki T, Murakami S, Matsubara N, Tanaka M, Yoshino T, Ota J, Nakagawa T, Ishihara Y, Ito T, Saito A, Yamaki K, Matsuzaki E, Hidaka T, Sasaki D, Yaegashi T, Yasuda T, Shibutani T, Noguchi K, Araki H, Ikumi N, Aoyama Y, Kogai H, Nemoto K, Deguchi S, Takiguchi T, Yamamoto M, Inokuchi K, Ito T, Kado T, Furuichi Y, Kanazashi M, Gomi K, Takagi Y, Kubokawa K, Yoshinari N, Hasegawa Y, Hirose T, Sase T, Arita H, Kodama T, Shin K, Izumi Y, Yoshie H. Prevalence and risk factors for peri-implant diseases in Japanese adult dental patients. J Oral Sci 2017; 59: 1-11.
9) Romito GA, Hassan MA, Do Amaral GCLS, Villar CC. Decision-making on peri-implant

mucositis management and treatment approaches. Br Dent J. 2024; 236: 797-801.
10) Pereira R, Sabri H, Nava P, Alrmali A, Wang H-L. Treatment strategies for peri-implant mucositis: the final stop for preventing peri-implantitis. Int J Dent 2025: 2025: 6901156. doi: 10.1155/ijod/6901156.
11) Carinci F, Romanos GE, Scapoli L. Molecular tools for preventing and improving diagnosis of peri-implant diseases. Periodontol 2000. 2019; 81: 41-47.
12) Smeets R, Henningsen A, Jung O, Heiland M, Hammächer C, Stein JM. Definition, etiology, prevention and treatment of peri-implantitis - a review. Head Face Med 2014: 10: 34. doi: 10.1186/1746-160X-10-34.
13) Ramanauskaite A, Cafferata EA, Begic A, Schwarz F. Surgical interventions for the treatment of peri-implantitis. Clin Implant Dent Rel Res 2022; 25: 682–695.
14) Mahato N, Wu X, Wang L. Management of peri-implantitis: a systematic review, 2010-2015. Springerplus 2016: 5: 105. doi: 10.1186/s40064-016-1735-2.
15) Renvert S, Roos‐Jansåker A, Claffey N. Non‐surgical treatment of peri‐implant mucositis and peri‐implantitis: a literature review. J Clinic Periodontology 2008; 35: 305-315.
16) Sahm N, Becker J, Santel T, Schwarz F. Non-surgical treatment of peri-implantitis using an air-abrasive device or mechanical debridement and local application of chlorhexidine: a prospective, randomized, controlled clinical study. J Clinical Periodontol 2011; 38: 872-878.
17) Moharrami M, Perrotti V, Iaculli F, Love RM, Quaranta A. Effects of air abrasive decontamination on titanium surfaces: A systematic review of in vitro studies. Clin Implant Dent Rel Res 2019; 21: 398-421.
18) El Chaar E, Almogahwi M, Abdalkader K, Alshehri A, Cruz S, Ricci J. Decontamination of the infected implant surface: a scanning electron microscope study. Int J Periodontics Restorative Dent 2020; 40: 395-401.
19) Lollobrigida M, Fortunato L, Serafini G, Mazzucchi G, Bozzuto G, Molinari A, Serra E, Menchini F, Vozza I, De Biase A. The prevention of implant surface alterations in the treatment of peri-implantitis: comparison of three different mechanical and physical treatments. Int J Environ Res Public Health 2020; 17: 2624. doi: 10.3390/ijerph17082624.
20) Schou S, Holmstrup P, Jørgensen T, Skovgaard LT, Stoltze K, Hjørting‐Hansen E, Wenzel A. Implant surface preparation in the surgical treatment of experimental peri-implantitis with autogenous bone graft and ePTFE membrane in cynomolgus monkeys. Clinical Oral Implants Res 2003; 14: 412-422.
21) Ronay V, Merlini A, Attin T, Schmidlin PR, Sahrmann P. In vitro cleaning potential of three implant debridement methods. Simulation of the non-surgical approach. Clinical Oral Implants Res 2016; 28: 151-155.
22) Sato H, Ishihata H, Kameyama Y, Shimpo R, Komasa S. Professional mechanical tooth cleaning method for dental implant surface by agar particle blasting. Materials (Basel). 2021; 14(22): 6805. doi: 10.3390/ma14226805.
23) Hirota M, Mochizuki C, Sakurai T, Mishima H, Ohkubo C, Yamamoto T. Development of a sustainable bone regeneration material using apatite paste derived from eggshell waste. J Funct Biomater 2025; 16(6): 201. doi: 10.3390/jfb16060201.
24) Ding Z, Cheng W, Liu L, Xu G, Lu Q, Kaplan DL. Nanosized silk-magnesium complexes for tissue regeneration. Adv Healthcare Mater 2023; 12(26): e2300887. doi: 10.1002/adhm.202300887.
25) Da Silva JG, Babb R, Salzlechner C, Sharpe PT, Brauer DS, Gentleman E. Optimisation of lithium-substituted bioactive glasses to tailor cell response for hard tissue repair. J Mater Sci 2017; 52: 8832-8844.
26) Mellado-Valero A, Buitrago-Vera P, Solá-Ruiz MF, Ferrer-García JC. Decontamination of dental implant surface in peri-implantitis treatment: A literature review. Med Oral 2013; 18: e869-e876.
27) Monje A, Pons R, Peña P. Electrolytic surface decontamination in the reconstructive therapy of peri-implantitis: single-center outcomes. Int J Periodontics Restorative Dent 2024; 45: 1-23.
28) Schwarz F, Hegewald A, John G, Sahm N, Becker J. Four‐year follow‐up of combined surgical therapy of advanced peri‐implantitis evaluating two methods of surface decontamination. J Clinic Periodontology 2013; 40: 962-967.
29) Schwarz F, John G, Schmucker A, Sahm N, Becker J. Combined surgical therapy of advanced peri-implantitis evaluating two methods of surface decontamination: a 7-year follow-up observation. J Clinic Periodontology 2017; 44: 337-342.
30) Schwarz F, John G, Mainusch S, Sahm N, Becker J. Combined surgical therapy of peri-implantitis evaluating two methods of surface debridement and decontamination. A two-year clinical follow up report. J Clinic Periodontology 2012; 39: 789-797.
31) Pisano M, Amato A, Sammartino P, Iandolo A, Martina S, Caggiano M. Laser Therapy in the Treatment of Peri-Implantitis: State-of-the-Art, Literature Review and Meta-Analysis. Appl Sci 2021; 11(11): 5290; https://doi.org/10.3390/app11115290
32) Schwarz F, Sahm N, Iglhaut G, Becker J. Im-

pact of the method of surface debridement and decontamination on the clinical outcome following combined surgical therapy of peri-implantitis: a randomized controlled clinical study. Journal of Clinical Periodontology 2011; 38: 276-284.
33) Froum SJ, Dagba AS, Shi Y, Perez-Asenjo A, Rosen PS, Wang WCW. Successful surgical protocols in the treatment of peri-implantitis: a narrative review of the literature. Implant Dentistry 2016; 25: 416-426.
34) Ungvári K, Pelsöczi IK, Kormos B, Oszkó A, Rakonczay Z, Kemény L, Radnai M, Nagy K, Fazekas A, Turzó K. Effects on titanium implant surfaces of chemical agents used for the treatment of peri -implantitis. J Biomed Mater Res 2010; 94: 222-229.
35) Pereira MMA, De Molon RS, Barão VAR, Shibli JA, Sculean A, Pirih FQ, de Avila ED. Surveying coating strategies for peri-implantitis management: Clinical implications and classificatory approaches. J Periodontol 2025; 96: 1077-1087.
36) Mistry S, Kundu D, Datta S, Basu D. Comparison of bioactive glass coated and hydroxyapatite coated titanium dental implants in the human jaw bone. Australian Dent J 2011; 56: 68-75.
37) Park J, Kwon T, Suh J. The relative effect of surface strontium chemistry and superhydrophilicity on the early osseointegration of moderately rough titanium surface in the rabbit femur. Clinical Oral Implants Res 2012; 24: 706-709.
38) Ostrowski N, Lee B, Hong D, Enick PN, Roy A, Kumta PN. Synthesis, Osteoblast, and osteoclast viability of amorphous and crystalline tri-magnesium phosphate. ACS Biomater Sci Eng 2014; 1: 52-63.
39) Agour M, Abdal-Hay A, Hassan MK, Bartnikowski M, Ivanovski S. Alkali-treated titanium coated with a polyurethane, magnesium and hydroxyapatite composite for bone tissue engineering. Nanomaterials (Basel) 2021; 11(5): 1129. doi: 10.3390/nano 11051129.
40) Blair HC, Larrouture QC, Tourkova IL, Liu L, Bian JH, Stolz DB, Nelson DJ, Schlesinger PH. Support of bone mineral deposition by regulation of pH. Am J Physiol Cell Physiol 2018; 315(4): C587-C597. doi: 10.1152/ajpcell. 00056.2018.
41) Boonrungsiman S, Gentleman E, Carzaniga R, Evans ND, Mccomb DW, Porter AE, Stevens MM. The role of intracellular calcium phosphate in osteoblast-mediated bone apatite formation. Proc Natl Acad Sci USA. 2012; 109: 14170-14175.

(Received: May 8, 2026/
Accepted: June 26, 2026)

Corresponding author:
Satoshi Komasa, D.D.S.,Ph.D
Department of Oral Health Sciences
Faculty of health Sciences,
Osaka Dental University
1-4-4 Makino-honmachi, Hirakata-shi,
Osaka 573-1121, Japan
Tel:＋81-72-856-9975
Fax:＋81-72-856-9413
E-mail: komasa-s@cc.osaka-dent.ac.jp